Journal of the American Ceramic Society

Volume 91 Issue 1 Page 329-332, January 2008

To cite this article: Aparna Mondal, Shanker Ram (2008) Enhanced Phase Stability and Photoluminescence of Eu^{3+} Modified *t*-ZrO_2 Nanoparticles Journal of the American Ceramic Society

91 (1) , 329–332

http://dx.doi.org/10.1111/j.1551-2916.2007.02137.x

Enhanced Phase Stability and Photoluminescence of Eu^{3+} Modified t-ZrO_2 Nanoparticles

Aparna Mondal[*†] and Shanker Ram[‡]

Department of Chemistry, National Institute of Technology, Rourkela – 769008, Orissa, India, and
Materials Science Centre, Indian Institute of Technology, Kharagpur - 721302, India

[*]Corresponding author, Fax: (+91)-661-2462999, E-mail: aparnamondal@gmail.com

[†] National Institute of Technology

[‡] Indian Institute of Technology

Abstract

Tetragonal (t) ZrO_2 of nanoparticles, have been achieved by a partial $Eu^{3+} \rightarrow Zr^{4+}$ substitution, synthesized using a simple oxalate method at a moderate temperature of 650°C in air. The Eu^{3+} additive, 2 mol% used according to the optimal photoluminescence (PL), renders small crystallites of the sample. On raising the temperature further, average crystallite size D grows slowly from 16 nm to a value as big as 49 nm at 1200°C. The Eu^{3+}:t-ZrO_2 nanoparticles have a wide PL spectrum at room temperature in the visible to near IR regions (550 - 730 nm) in the $^5D_0 \rightarrow {}^7F_J$ (Eu^{3+}), J = 1 to 4, electronic transitions. The intensity of $^5D_0 \rightarrow {}^7F_4$ group is as large as the characteristic $^5D_0 \rightarrow {}^7F_2$ group of the spectrum in the forced electric-dipole allowed transitions. The enhanced t-ZrO_2 phase stability and wide PL can be attributed to the combined effects of an amorphous Eu^{3+}-rich surface and part of the Eu^{3+} doping of ZrO_2 of small crystallites.

Key words: Chemical Synthesis; Oxalate processing; Eu^{3+}:t-ZrO_2 nanopowder; Phase stability in small particles; Tetragonal ZrO_2; X-ray diffraction; Photoluminescence.

I. Introduction

Nanocrystalline t-ZrO_2 has extensive use as catalysts or catalyst supports,[1,2] and as oxygen sensor.[3] It is known to have excellent mechanical properties and one of the so called 'superplastic' structural materials.[3-5] Doped t-ZrO_2 with rare-earth ions can be employed as building blocks to develop a wide range of nanotechnological optical materials due to its chemical and physical stability, high refractive index, and low phonon energy.[2,6-9] At atmospheric pressure, bulk ZrO_2 exists in three well-known polymorphs of $P2_1/c$ monoclinic (m), $P4_2/nmc$ tetragonal (t), and Fm3m cubic fluorite (c) crystal structures, with m-ZrO_2 the equilibrium structure at low temperatures.[2,5] The *t*- or *c*-ZrO_2 appears upon heating m-ZrO_2 to 1170ºC or 2370ºC.[2,5]

A chemical doping of divalent and trivalent cations such as Mg^{2+}, Ca^{2+}, Cr^{3+}/Cr^{4+}, or rare-earth ions was used to obtain the c- and t-ZrO_2 phases at low temperature.[5,8-10] Small particle size, dopands, and possible O^{2-} vacancies lead the system to the increase in the Gibbs free energy to cope with the values for such polymorphs. Part of the dopand segregates, forming a high-energy surface-strained core-shell structure of particles.[10] According to phase stability, at a certain critical temperature, m-ZrO_2 reverts back after relieving the excess energy.

The t-ZrO_2 in form of nanoparticles has been prepared at low temperature by several methods including polymer template,[2] sol-gel,[9,11] microwave irradiation,[7] or precipitation.[4,10,12] 3 mol% Y^{3+} stabilized t-ZrO_2 of nanophase, prepared via an oxalate method, retains well up to 650°C.[13] In doped or coated t-ZrO_2 particles with 1 mol % Eu^{3+}, a mixed phase develops with m-ZrO_2 as early as 1000°C.[8,12] A single t-ZrO_2 phase was retained with as large as 9.4 mol % Eu_2O_3.[14] There is a growing demand for producing stable t-ZrO_2 with minimal doping. Few studies have been carried out concerning photoluminescence (PL) properties of nanoscale rare earth doped ZrO_2 crystallites.[6,7,,8] PL has renewed the interest in Eu^{3+} :t-ZrO_2 nanoparticles to discover its potential applications. Here, we apply a simple oxalate method for synthesizing such nanoparticles, with a wide PL from 550 to 730 nm. Eu^{3+} doping as small as 2 mol% renders a single t-phase to be stable up to a temperature as high as 1200°C in air.

II. Experimental Procedure

$ZrOCl_2 \cdot 8H_2O$, Eu_2O_3, and oxalic acid of 99.99 % purity were used as raw materials. Aqueous solutions (1.0 M) of $ZrOCl_2 \cdot 8H_2O$ and oxalic acid were prepared. A requisite amount of Eu_2O_3 (0.02 M/dl in HCl) was admixed to the $ZrOCl_2 \cdot 8H_2O$ solution and then the oxalic acid was added drop-wise to perform the reaction by stirring with a magnetic stirrer at room temperature. The molar ratio of the (Eu + Zr)/oxalic acid solution was 1/1. The obtained gelly product of Eu-Zr oxalates was filtered and washed with distilled water to remove chlorides and other byproducts. Nanophase Eu^{3+}:t-ZrO_2 was formed after heating a dried (at 200ºC in air) and pulverized powder at 650°C for 2 h in air.

The Eu^{3+}:t-ZrO_2 structure was analyzed with X-ray diffraction (XRD). The XRD was recorded on a Philips P.W. 1710 X-ray diffractometer with 0.15418 nm CuKα radiation. Average D-value was calculated from the peak broadening with the Debye-Scherrer relation. A Jobin-Yvon Ramnor-HG-2S spectrophotometer was used to study Raman spectra by exciting the samples at 488.0 nm of an Ar^+ laser. The microstructure was studied using a JEOL JEM-200C transmission electron microscope (TEM). The PL was obtained by irradiating the sample at 465.8 nm of an Ar^+-ion laser, with 90 mW power and 3.0

mm beam diameter. A monochromator (SPEX model 500M) of a 600 lines/mm grating and an InGaAs detector collected the data.

III. Results and Discussion

Figure 1 shows XRD pattern of a typical sample 2 mol% Eu^{3+}:ZrO_2 after heating the oxalate at (a) 650ºC, (b) 1000ºC, and (c) 1200ºC in air for 2 h. As marked therein all the peaks belong to a single phase t-ZrO_2. Broad and asymmetric peaks in small crystallites, D = 16 nm, of powder (a) are distinguished to those of c-ZrO_2 with a close observation of the splitting in some of the peaks and the appearance of the (103) and (211) peaks. Such peaks are well resolved in symmetric and narrowed profiles in other two samples with 29 and 49 nm D-values, respectively. As portrayed in Fig. 2, the lattice parameters *a* and *c* changed as much as 0.3 and 0.6 %, respectively, on raising the temperature from 650 to 1200°C, with a = 0.3587 nm and c = 0.5150 nm after 650°C while a = 0.3599 nm and c = 0.5180 nm after 1200°C. Tetragonality $\tau = c/a$ improved from 1.436 to 1.439 (Fig. 2a). At early temperatures below 800°C, primarily the *a*-value continues to be increasing followed by the c-value so that τ-value decreases until it approaches 800°C and then rises rapidly, with no much change after 1000°C. Preferably, Eu^{3+} occupies the sites primarily along the *a*-axis at temperatures below 800°C while along the c-axis at higher values.

As plotted in the inset (b) to Fig. 2, the lattice volume V_o is increasing nonlinearly against the temperature, which is typical of a high-energy microstructure. A value of 0.06708 nm^3, which is larger than the 0.06678 nm^3 value in undoped t-ZrO_2 [15], is achieved after 2 h of heating at 1200°C. It is 1.2% larger than the value obtained in the sample heated at 650°C for 2 h in air.

An undoped sample heated at 500°C consists of both t- and m-ZrO_2 phases. Mostly the m-ZrO_2 develops as early as 650°C. The doping of 2 mol % Eu^{3+} by the oxalate route shifts the t $\rightarrow$ m-ZrO_2 transformation dramatically at temperature as high as 1450°C. As reported by Gutzov *et al.*[12], only a mixture of the two phases persists for 1 mol% Eu^{3+} doped ZrO_2 samples, obtained by the coprecipitaton from the $ZrOCl_2 \cdot 8H_2O$ and $Eu(NO_3)_3$ with NH_4OH in water and followed by calcining at over 350-1000°C. A coprecipitate containing even a larger Eu_2O_3 content of 6.4 mol% evolves a similar t-/m-ZrO_2 mixture up to a temperature of 1300°C.[14] In the equilibrium ZrO_2-Eu_2O_3 phase diagram, t-ZrO_2 occurs in a single phase compound over a limited Eu^{3+} content 3.0 mol% or lower after heating at and above 850°C.[16] Andrievskaya and Lopato proposed a non-equilibrium phase-diagram (metastable phase

diagram) based on XRD data at room temperature.[16] According to it, the metastable t-phase of ZrO_2 is stabilized by a narrow range of 3-6 mol% Eu_2O_3 after heating a precipitate at 1170°C in air.

The Eu^{3+}:t-ZrO_2 phase is characterized further with its distinctive Raman spectrum, which shows six normal modes of vibration A_{1g}, $2B_{1g}$, and $3E_g$.[2,17] It differs from the c-ZrO_2, which has only one Raman active band F_{2g}. Figure 3 shows a typical spectrum for the sample Eu^{3+}:t-ZrO_2 heated at 650°C for 2 h. The six bands at 150, 265, 318, 468, 609 and 640 cm^{-1} are very similar to the values for undoped t-ZrO_2.[17] In general, the present values stand 5-15 cm^{-1} larger in the modified force fields in the presence of Eu^{3+} ions and/or possible O^{2-} vacancies. The TEM images in Fig. 4a reveal the particles of 13 to 65 nm diameters self-assembled in a specific structure with enclosed pores in between the particles. Some of the particles (dark) accompany distinct thin surface layers with rather less darkness. Average lattice spacing in the high resolution lattice images in Fig. 4b is 0.2925 nm, which is in proximity to the value of 0.2931 nm of the (101) reflection in XRD in Fig. 1. In the top corner in Fig. 4b, a cation column with a markedly low level of intensity is denoted by an arrow. In the vicinity, one observes a strong deviation from the image contrast of the perfect structure, possibly due to deficiency of Zr^{4+}, i.e., presumably the $Eu^{3+} \rightarrow Zr^{4+}$ substitution. A distinct amorphous surface layer (denoted as a-layer) is very much visible in Fig. 4b.

There are reasons to believe that part of the Eu^{3+} used forms the Eu^{3+}:t-ZrO_2 surface layer with controlled D-value of the surface modified crystallites. This let the structure survive in extended D-values up to 49 nm, which is well above the critical value of D_c = 30 nm for pure t-ZrO_2[18] stabilization. Shukla *et al.*[19] observed similarly large spherical particles (45 nm) of pure ZrO_2, which exhibits t-phase at room temperature. The tendency of nanocrystallites to form hard-aggregates is observed to be responsible for stabilizing within the large sized ZrO_2 particles in the range of 500-600 nm. In the thermodynamics[5,10], the D_c value depends on the particle surfaces, interfacial energy, strain energy, and the volume Gibbs free energy (affected by the vacancies and the local site symmetries).

As shown in Fig. 5, a typical sample Eu^{3+}:t-ZrO_2 consists of four PL bandgroups (i) 560 - 600, (ii) 600 - 645, (iii) 645 - 680, and (iv) 680 - 730 nm in the $^5D_0 \rightarrow {}^7F_1$, $^5D_0 \rightarrow {}^7F_2$, $^5D_0 \rightarrow {}^7F_3$, and $^5D_0 \rightarrow {}^7F_4$ (Eu^{3+}) transitions, respectively. The peak intensities of the representative members are in the ratio of 63: 100: 34: 87. Characteristically weak $^5D_0 \rightarrow {}^7F_0$ band has no visible value. The $^5D_0 \rightarrow {}^7F_1$ (592 nm) band, which is a magnetic-dipole allowed transition,[20,21] has a relatively enhanced value. The $^5D_0 \rightarrow {}^7F_3$ (658 nm) band, a forbidden transition by the electric-dipole as well as the magnetic-dipole[20], appears to

be the weakest band of the spectrum. As a hypersensitive forced electric-dipole transition, the $^5D_0 \rightarrow {}^7F_2$ (608 nm) band stands to be the predominant group in the $^5D_0 \rightarrow {}^7F_J$, $J = 0 \rightarrow 4$, series. The implication is that Eu^{3+} occupies the sites of presumably distorted symmetries in the Eu^{3+}:t-ZrO_2 nanocomposite particles.

Unusually, the $^5D_0 \rightarrow {}^7F_4$ (714 nm) transition (forced electric-dipole[20]) represents the second most intense bandgroup in this example of Eu^{3+}:t-ZrO_2 nanoparticles. Eu_2O_3 doped or coated sample of mostly m-ZrO_2, prepared by Ghosh and Patra[8], has no significant intensity in this transition. Two prominent bands at 596 and 617 nm were observed in such samples annealed at 1000 and 1100°C.[8] The Eu^{3+}-Eu^{3+} ionic and electron–phonon interactions are a function of the microstructure in tuning the spectrum sensitively according to the local and the long range structures of hybrid composite nanoparticles. Presence of small pores is another important issue to control such interactions.[10,21] Small particles and intergranular Eu^{3+} doping of Eu^{3+}:ZrO_2, with a huge strain, thus seems to be a major source of inducing the optical properties.

IV. Conclusions

Metastable t-ZrO_2 has been successfully synthesized using oxalate method with as small doping as 2 mol% Eu^{3+}. This synthesis route provides a simple and economic method in comparison with the sol-emulsion-gel or other processes for producing t-ZrO_2 nanoparticles. The Eu^{3+}:t-ZrO_2 formation, stability, and PL properties were studied with the X-ray diffraction, microstructure and PL techniques. This specific phase stands to be stable up to a temperature as high as 1200°C in air. The grain surface, the internal distribution of Eu^{3+} within the Eu^{3+}:t-ZrO_2 lattice, and possible O^{2-} vacancies play important role in stabilizing this phase, with a wide and intense PL in the visible-near IR regions. The results suggest that Eu^{3+}:t-ZrO_2 nanoparticles can be used as building blocks to develop a wide range of nanomaterials for photonics and other devices.

Acknowledgements: The work was partly supported with funds of the Defense Research & Development Organization (DRDO), Government of India.

References

[1]Y. W. Li, D. H. He, Z. X. Cheng, C. L. Su, J. R. Li, and M. J. Zhu, "Effect of Calcium Salts on Isosynthesis over ZrO_2 Catalysts," *Mol. Catal. A,* **175** [1-2] 267-75 (2001).

[2]J. Cao, X. Qiu, B. Luo, Y. Liang, Y. Zhang, R. Tan, M. Zhao, and Q. Zhu, "Synthesis and Room-Temperature Ultraviolet Photoluminescence Properties of Zirconia Nanowires," *Adv. Funct. Mater.,* **14** [3] 243-46 (2004).

[3]I-W. Chen, and L. A Xue, "Development of Superplastic Structural Ceramics," *J. Am. Ceram. Soc.,* **73** [9] 2585-2609 (1990).

[4]Nae-Lih Wu, and Ton-Fon Wu, "Enhanced Phase Stability for Tetragonal Zirconia in Precipitation Synthesis," *J. Am. Ceram. Soc.,* **83** [12] 3225-27 (2000).

[5]A. Mondal, and S. Ram, "A Monolithic c-ZrO_2 Nanopowder through an Energized $ZrO(OH)_2{\cdot}xH_2O$ Polymer Precursor," *J. Am. Ceram. Soc.,* **87** [12] 2187–94 (2004).

[6]R. Reisfeld, M. Zelner, and A. Patra, **"**Fluorescence Study of Zirconia Films Doped by Eu^{3+}, Tb^{3+} and Sm^{3+} and Their Comparison with Silica Films", *J. Alloys and Compd.,* **300-301** 147-151 (2000).

[7]J. Liang, Z. Deng, X. Jiang, F. Li, and Y. Li, "Photoluminescence of Tetragonal ZrO_2 Nanoparticles Synthesized by Microwave Irradiation," *Inorg. Chem.,* **41** [14] 3602-04 (2002).

[8]P. Ghosh, and A. Patra, "Role of Surface Coating in ZrO_2/Eu^{3+} Nanocrystals**,"** *Langmuir,* **22** [14] 6321-27 (2006).

[9]M. Mizuno, Y. Sasaki, S. Lee, and H. Katakura, "High-Yield Sol-Gel Synthesis of Well-Dispersed, Colorless ZrO_2 Nanocrystals," *Langmuir,* **22** [17] 7137-7140 (2006).

[10]S. Ram, "Synthesis and Structural and Optical Properties of Metastable ZrO_2 Nanoparticles with Intergranular Cr^{3+}/Cr^{4+} Doping and Grain Surface Modification," *J. Mater. Sci.*, **38** 643-55 (2003).

[11]C. N. Chervin, B. J. Clapsaddle, H. W. Chiu, A. E. Gash, J. H. Satcher, and S. M. Jr., Kauzlarich, "Aerogel Synthesis of Yttria-Stabilized Zirconia by a Non-Alkoxide Sol-Gel Route," *Chem. Mater.*, **17** [13] 3345-51 (2005).

[12]S. Gutzov, J. Ponahlo, C. L. Lengauer, and A. Beran, "Phase Characterization of Precipitated Zirconia," *J. Am. Ceram. Soc.*, **77** [7] 1649-52 (1994).

[13]O. Vasylkiv, Y. Sakka, and H. Borodians'ka, "Nonisothermal Synthesis of Yttria-Stabilized Zirconia Nanopowder through Oxalate Processing: II, Morphology Manipulation," *J. Am. Ceram. Soc.,* **84** [11] 2484-88 (2001).

[14]D. A. Moore, and I. F. Ferguson, "Zirconia-Stabilized Cubic Europia," *J. Am. Ceram. Soc.*, **65** [9] 414-18 (1982).

[15]*X-ray Powder Diffraction Files JCPDS-ICDD* (Joint Committee on Powder Diffraction Standards), (International Centre for Diffraction Data, Swarthmore, PA,1999), (a) 27-0997, c-ZrO_2, (b) 79-1771, t-ZrO_2, and (c) 13-0307, m-ZrO_2.

[16]E. R. Andrievskaya, and L. M. Lopato, "Influence of Composition on the T→M Transformation in the Systems ZrO_2-Ln_2O_3 (Ln = La, Nd, Sm, Eu)," *J. Mater. Sci.,* **311** 2591-96 (1995).

[17]G.-M. Rignanese, F. Detraux, and X. Gonze, "First-principles Study of Dynamical and Dielectric Properties of Tetragonal Zirconia," *Phys. Rev. B,* **64** 134301-07 (2001).

[18]R. C. Garvie, "The Occurrence of Metastable Tetragonal Zirconia as a Crystallite Size Effect," *J. Phys. Chem.*, **69** [4] 1238-43 (1965).

[19]S. Shukla, S. Seal, R. Vij, S. Bandyopadhyay, and Z. Rahman, "Effect of Nanocrystallite Morphology on the Metastable Tetragonal Phase Stabilization in Zirconia," *Nano Lett.* **2** 989-93 (2002).

[20]K.A. Gschneid Jr. and L. R. Eyring, *Handbook on the Physics and Chemistry on Rare-earths*, Vol. 3, North-Holland, Amsteram (1979).

[21]P. Mohanty, and S. Ram, "Light Emission Associated with the $^5D_0 \rightarrow {}^7F_3$ Forbidden Transition in Eu^{3+} Cations Dispersed in an Eu^{3+} :Al_2O_3 Mesoporous Structure," *Philos. Magn. Lett.*, **86** [6] 375-84 (2006).

Figure captions

Fig. 1. X-ray diffractograms of Eu^{3+}: t-ZrO_2 after heating an oxalate precursor at (a) 650°C, (b) 1000°C, and (c) 1200°C in air for 2 h.

Fig. 2. Variations in the *a* and *c*-values in Eu^{3+}: t-ZrO_2 as a function of the processing temperature. The plots for *c*/*a* and V_o are given in the insets (a) and (b) respectively.

Fig. 3. Raman spectrum of Eu^{3+}: t-ZrO_2 heated at 650°C for 2 h in air.* Electronic Raman band.

Fig. 4. (a) TEM and (b) lattice images of Eu^{3+}: t-ZrO_2 heated at 650°C for 2 h in air.

Fig. 5. PL of Eu^{3+}: t-ZrO_2 heated at 650°C for 2 h in air.

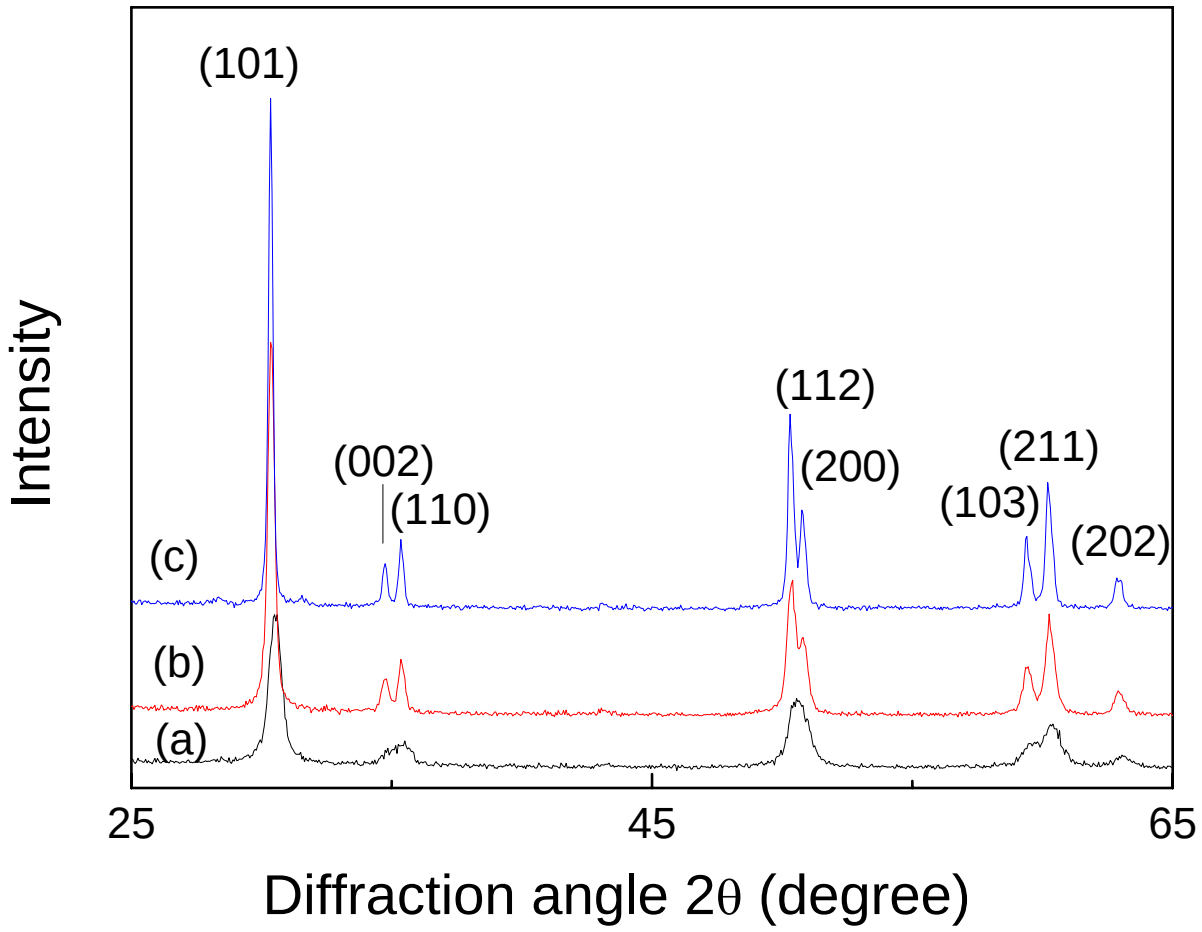

Fig. 1. X-ray diffractograms of Eu^{3+}: t-ZrO_2 after heating an oxalate precursor at (a) 650°C, (b) 1000°C, and (c) 1200°C in air for 2 h.

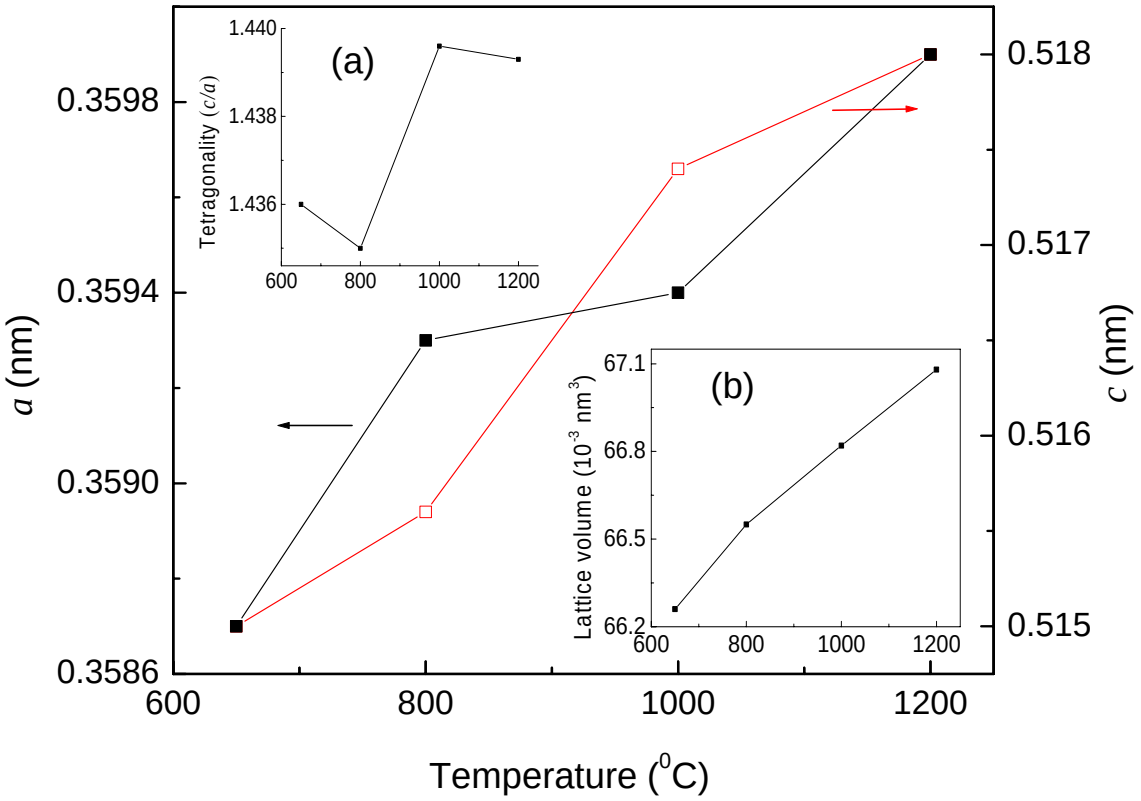

Fig. 2. Variations in the *a* and *c*-values in Eu^{3+}: t-ZrO_2 as a function of the processing temperature. The plots for *c*/*a* and V_o are given in the insets (a) and (b) respectively.

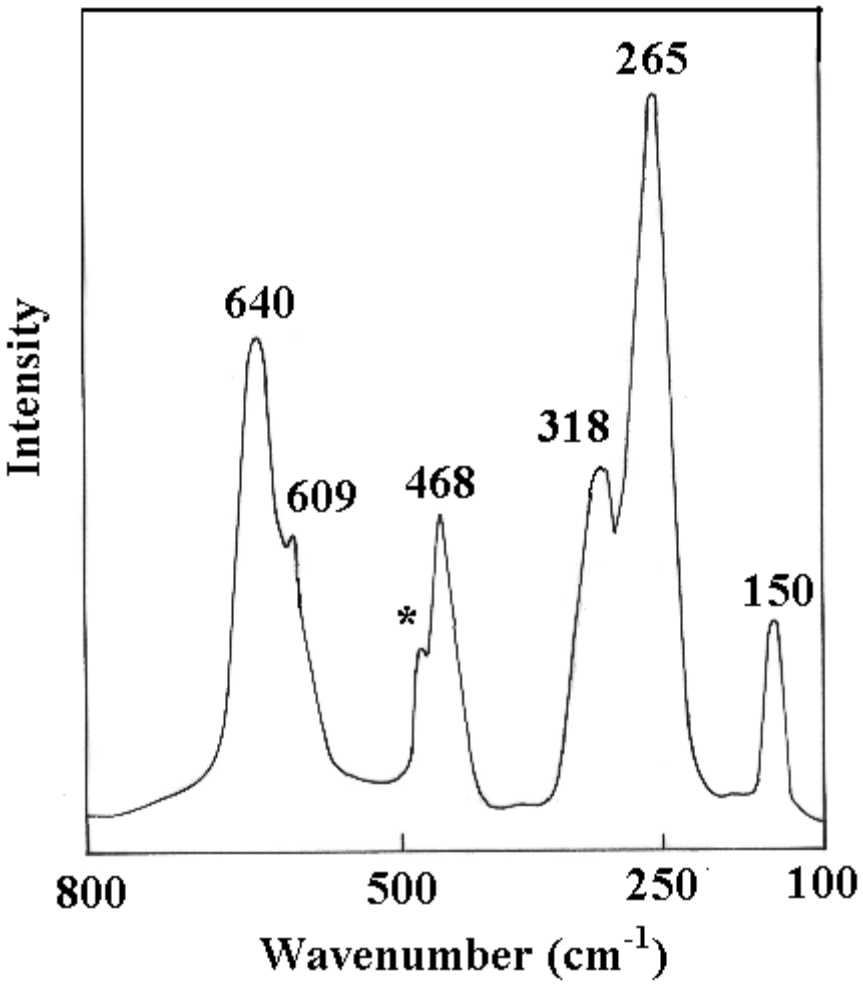

Fig. 3. Raman spectrum of Eu^{3+}: t-ZrO_2 heated at 650°C for 2 h in air.* Electronic Raman band.

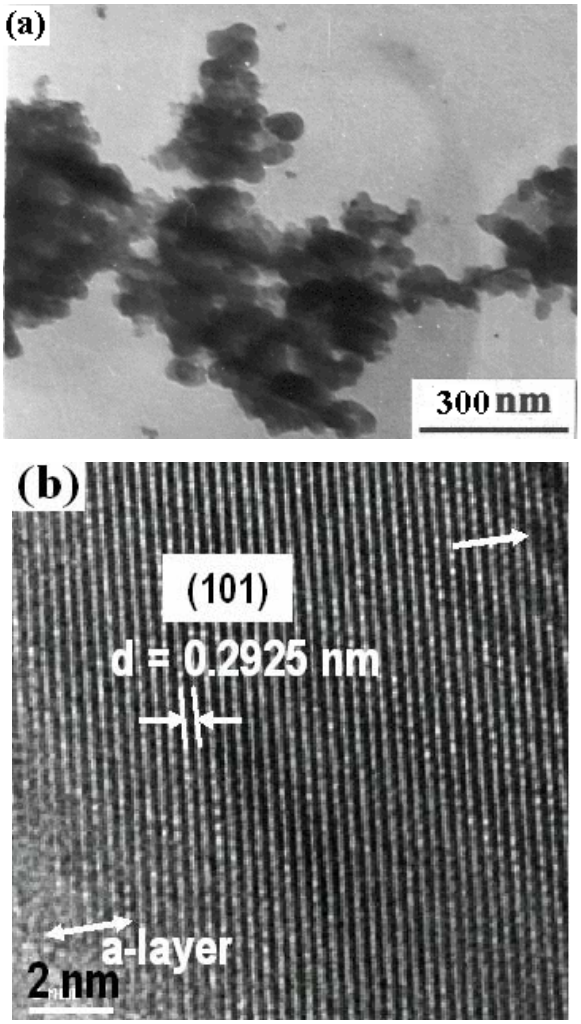

Fig. 4. (a) TEM and (b) lattice images of Eu^{3+}: t-ZrO_2 heated at 650°C for 2 h in air.

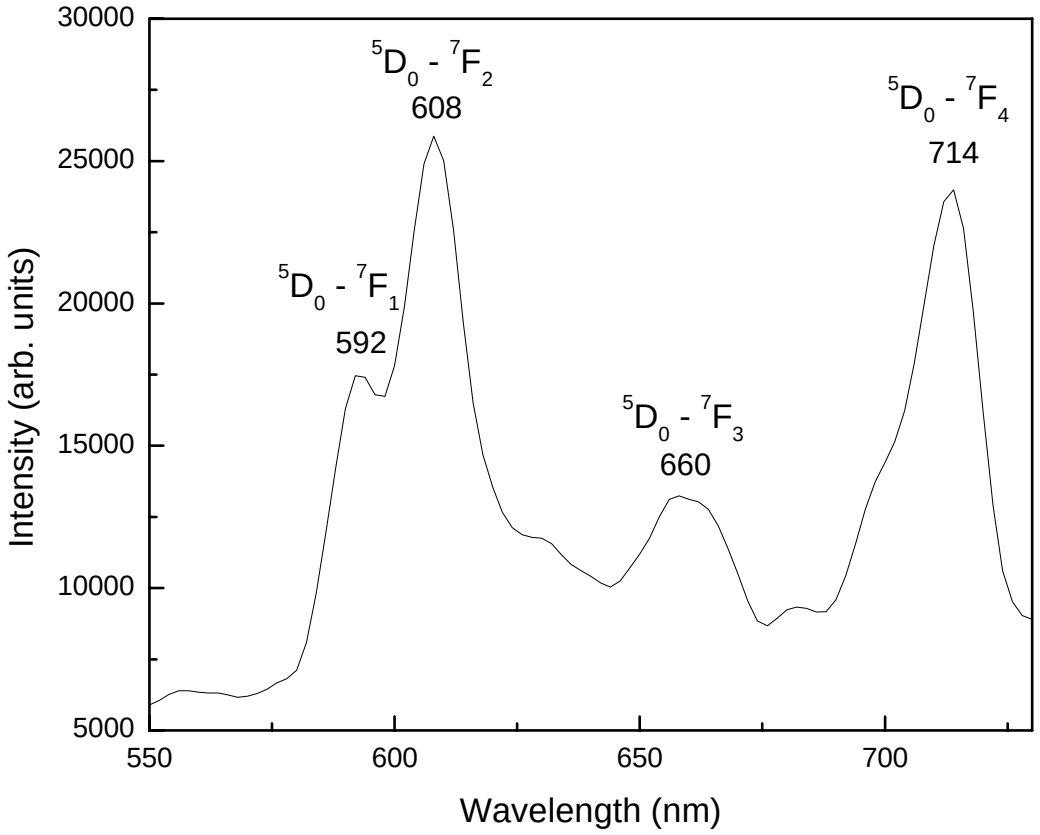

Fig. 5. PL of Eu^{3+}: t-ZrO_2 heated at 650°C for 2 h in air.